JB
Journals.ASM.org

The *Yersinia pestis* Rcs Phosphorelay Inhibits Biofilm Formation by Repressing Transcription of the Diguanylate Cyclase Gene *hmsT*

Yi-Cheng Sun,[a,b,c] Xiao-Peng Guo,[a] B. Joseph Hinnebusch,[b] and Creg Darby[c]

MOH Key Laboratory of Systems Biology of Pathogens, Institute of Pathogen Biology, Chinese Academy of Medical Sciences and Peking Union Medical College, Beijing, China[a]; Laboratory of Zoonotic Pathogens, Rocky Mountain Laboratories, National Institute of Allergy and Infectious Diseases, National Institutes of Health, Hamilton, Montana, USA[b]; and Department of Cell & Tissue Biology, Program in Microbial Pathogenesis and Host Response, University of California, San Francisco, San Francisco, California, USA[c]

***Yersinia pestis*, which causes bubonic plague, forms biofilms in fleas, its insect vectors, as a means to enhance transmission. Biofilm development is positively regulated by *hmsT*, encoding a diguanylate cyclase that synthesizes the bacterial second messenger cyclic-di-GMP. Biofilm development is negatively regulated by the Rcs phosphorelay signal transduction system. In this study, we show that Rcs-negative regulation is accomplished by repressing transcription of *hmsT*.**

Yersinia pestis, the agent of bubonic plague, infects fleas, its vectors, by producing bacterial biofilms that can colonize the insect foregut (19). Growth of the biofilm interferes with blood feeding by the infected fleas and potentiates regurgitative transmission. Complete blockage of the foregut by the bacterial biofilm can occur, and blocked fleas bite mammals repeatedly in futile feeding attempts, further enhancing transmission. *Y. pestis* biofilms, in which bacteria are surrounded by a self-synthesized polysaccharide-rich matrix, appear to be made only when the bacteria colonize fleas. Several proteins required for *Y. pestis* biofilms are proteolytically degraded at mammalian body temperatures (25), *in vitro* biofilms are greatly diminished at 37°C, and a *Y. pestis* strain defective for biofilm genes was nevertheless highly virulent in a mouse infection (3, 22, 32).

Y. pestis biofilms are positively regulated by cyclic-di-GMP (c-di-GMP), which is synthesized by diguanylate cyclase (DGC) enzymes. The *Y. pestis* genome encodes several putative DGCs, but only two of them, HmsT and Y3730, are related to biofilm formation (3, 8, 22, 32). *Yersinia pseudotuberculosis*, a bacterium closely related to *Y. pestis*, also makes biofilms that are regulated by *hmsT* (10). The biofilm-promoting activity of c-di-GMP has not been determined, but in other systems, c-di-GMP has been shown to be an allosteric activator of glycosyltransferases (27, 28).

Y. pestis and *Y. pseudotuberculosis* biofilms are negatively regulated by the Rcs phosphorelay system (33). Rcs consists of two membrane-bound proteins, RcsC and RcsD, a DNA-binding response regulator, RcsB, and an accessory protein, RcsA. In phosphorelays of this type, outputs can be dependent on RcsB alone, acting in homodimers, or on heterodimers of RcsB and RcsA (23). Genetic investigation showed that in *Y. pestis*, *rcsA* is a nonfunctional pseudogene, while in *Y. pseudotuberculosis*, *rcsA* is functional and represses biofilms (33). Although *rcsD* has a frameshift in *Y.pestis*, it is still functional and may dephosphorylate RcsB to derepress biofilms (33).

The factors determining *hmsT* transcription have not been examined. In the present study, we show that in *Y. pestis* and *Y. pseudotuberculosis*, Rcs represses *hmsT* transcription.

MATERIALS AND METHODS

Bacterial strains and plasmids. The strains and plasmids used are shown in Table 1. CDY497 was made by a method to insert PCR products into the chromosome using the Red recombination system (11, 33). For strains containing Δ*lacZ*::Cm, the same method was used, after which reporter constructs containing *hmsP*::*lacZ* and *hmsH*::*lacZ* fusions were inserted by a modification of the Red method (17). In strains that are Δ*lacZ* but without chloramphenicol resistance (CDY622, CDY635, CDY636, CDY637, CDY638, and CDY639), the chloramphenicol resistance gene was cured (11). The RcsAB box mutation strains CDY983 and CDY984 were made by two-step allelic replacement (9, 12). A 1.5-kb PCR product containing the RcsAB box of *hmsT* was amplified from *Y. pestis* KIM6+ and cloned into pUC18. Using the resulting plasmid as the template, the CC dinucleotide was mutated to AG using a mutagenic PCR primer, and the product was substituted into the *Y. pestis* chromosome by allelic replacement (12). The oligonucleotide primers used are shown in Table S1 in the supplemental material. All strains were verified by PCR, DNA sequencing, or plasmid complementation, as appropriate.

***In vitro* biofilms.** Microtiter plate biofilm assays were carried out as previously described (32). Briefly, bacteria were grown in LB broth supplemented with 4 mM $CaCl_2$ and 4 mM $MgCl_2$ overnight at room temperature, diluted to an optical density at 600 nm (OD_{600}) of 0.02, and then aliquoted to 96-well polystyrene plates, which were incubated with shaking at 250 rpm for 24 h at room temperature. Media and planktonic cells were removed; the wells were washed, and the adherent biofilm was stained with crystal violet, which was subsequently solubilized with 80% ethanol–20% acetone before the A_{600} was measured. Background absorbance for uninoculated control wells was subtracted. Results from three independent experiments with five replicates per experiment were analyzed by one-way analysis of variance (ANOVA) with Dunnett's posttest to compare the wild type to the other strains.

***Caenorhabditis elegans* biofilms.** Biofilms were assayed for their ability to inhibit nematode growth as described previously (33). Briefly, adult *C. elegans* adults were allowed to lay eggs on lawns of bacteria for 2 to 4 h. After the adults were removed, the plates were incubated for 2 days at 20°C, and the worm development to the fourth larval (L4) stage was scored. Three independent experiments were carried out with at least 1,200 worms per sample.

Received 22 September 2011 Accepted 2 February 2012
Published ahead of print 10 February 2012
Address correspondence to Yi-Cheng Sun, sunyc@ipbcams.ac.cn.
Supplemental material for this article may be found at http://jb.asm.org/.

doi:10.1128/JB.06243-11

TABLE 1 Strains and plasmids used in this study

Strain or plasmid	Genotype and/or description	Reference or source
Strains		
Y. pestis		
KIM6+	Wild type (pCD1-)	14
CDY319	Δ*rcsD*::*kan*	33
CDY325	Δ*rcsB rcsD*::*kan*	33
CDY326	Δ*rcsB*::*kan*	33
CDY330	Δ*rcsA*::$rcsA_{YPSTB}$	33
CDY377	Δ*rcsD*::*kan* (pCBD190)	33
CDY421	Δ*rcsB*::*kan* Δ*rcsA*::$rcsA_{YPSTB}$	33
CDY475	KIM6+ (pCBD209)	This study
CDY497	Δ*hmsT*::*cat*	This study
CDY567	Δ*lacZ*::*cat hmsH*::*lacZ*	This study
CDY568	Δ*lacZ*::*cat hmsH*::*lacZ* Δ*rcsA*::$rcsA_{YPSTB}$	This study
CDY614	Δ*lacZ*::*cat hmsP*::*lacZ*	This study
CDY615	Δ*lacZ*::*cat hmsP*::*lacZ* Δ*rcsA*::$rcsA_{YPSTB}$	This study
CDY622	Δ*lacZ*	This study
CDY635	Δ*lacZ hmsT*::*lacZ*	This study
CDY636	Δ*lacZ hmsT*::*lacZ* (pCBD209)	This study
CDY637	Δ*lacZ hmsT*::*lacZ* (pBAD/Myc-His)	This study
CDY638	Δ*lacZ hmsT*::*lacZ* (pCBD178)	This study
CDY639	Δ*lacZ hmsT*::*lacZ* (pCBD179)	This study
CDY641	KIM6+ (pCBD253)	This study
CDY642	KIM6+ (pCBD254)	This study
CDY981	Δ*hmsT*::*cat* (pCBD26)	32
CDY982	Δ*rcsA*::$rcsA_{YPSTB}$ (pCBD26)	This study
CDY983	RcsAB*	This study
CDY984	Δ*rcsA*::$rcsA_{YPSTB}$ RcsAB*	This study
CDY1071	Δ*rcsA*::$rcsA_{YPSTB}$ Δ*lacZ hmsT*::*lacZ*	This study
SY743	KIM6+ (pYC219)	This study
SY744	KIM6+ (pYC220)	This study
Y. pseudotuberculosis		
IP32953	Wild type; serogroup O1	7
CDY564	Δ*rcsA*::$rcsA_{YPE}$	33
CDY985	IP32953(pCBD26)	This study
Plasmids		
pBAD/*Myc*-His	Expression vector	Invitrogen
pCBD26	*hmsT* in pCR2.1-TOPO	31
pCBD178	$rcsA_{YPE}$ in pUC18	33
pCBD179	$rcsA_{YPSTB}$ in pUC18	33
pCBD190	$rcsD_{YPSTB}$ in PET32a	33
pCBD209	*rcsB* in pBAD/*Myc*-His	This study
pCBD253	$rcsA_{YPSTB}$ in pMal-4x	This study
pCBD254	$rcsA_{YPE}$ in pMal-4x	This study
pCR2.1-TOPO	Cloning vector for PCR products	Invitrogen
pUC18	Cloning vector	35
pMal-c4x	Expression vector	NEB
pYC219	$rcsA_{YPE}$-His_6 in pUC18	This study
pYC220	$rcsA_{YPSTB}$-His_6 in pUC18	This study

β-Galactosidase assays. Lysates were prepared from cells with chromosomal *hmsT*::*lacZ*, *hmsH*::*lacZ*, or *hmsP*::*lacZ* (Table 1). β-Galactosidase activities were measured spectrophotometrically following cleavage of ONPG (4-nitrophenyl-β-D-galactopyranoside) at 37°C and are expressed in Miller units (24). Results from at least two independent experiments done in triplicate were analyzed by two-tailed Student's *t* test.

qRT-PCR. Quantitative real-time reverse transcription-PCR (qRT-PCR) was carried out as previously described (32). Briefly, cells were grown in LB broth overnight, diluted to an OD_{600} of 0.05, and grown in LB broth at room temperature to OD_{600} of about 0.8. Total RNA was isolated from cells with the RNeasy minikit (Qiagen). Residual DNA was removed by treatment with ribosomal DNase I (rDNase I) (Ambion) and confirmed by PCR. cDNA was synthesized from the RNA and used for quantitative PCR on an ABI Prism 7900 sequence detection system (TaqMan; Applied Biosystems). The quantity of mRNA was normalized relative to the quantity of the reference gene *crr* (y1485), whose expression level was not affected by *in vivo* or *in vitro* growth conditions (29). The ratio of the normalized quantity of *hmsT* mRNA in different strains to the normalized quantity in the wild-type samples was calculated. The primers and probe sets used are listed in Table S1 in the supplemental material. Results from three independent experiments done in triplicate were analyzed by one-way ANOVA with Bonferroni's test.

Western blotting. Procedures for Western blotting were performed essentially as described previously (31). For HmsT detection, proteins were separated on a 12% Bis-Tris polyacrylamide gel (Invitrogen) and blotted onto nitrocellulose. The immunoblots were probed with HmsT rabbit antibody (25). Following incubation of horseradish peroxidase (HRP)-conjugated goat anti-rabbit secondary antibody (Invitrogen), the immunoreactive proteins were detected with Immobilon Western HRP substrate (Millipore). For RcsA-His_6 detection, proteins were treated with 8 M urea and separated on a 15% SDS-PAGE gel and blotted onto polyvinylidene difluoride (PVDF) membrane. The immunoblots were further detected by anti-His antibody (Invitrogen) following the same protocol described above.

Transcription start site of *hmsT*. The transcription start site of the *hmsT* gene was determined by using the FirstChoice RLM-RACE (random amplification of cDNA ends) kit (Ambion) according to the manufacturer's instructions. Primer sequences are listed in Table S1 in the supplemental material.

Protein purification. The RcsB-His_6 expression plasmid pCBD209 was constructed by inserting a PCR-amplified *rcsB* fragment into pBAD/*Myc*-His vector (Invitrogen). Expression plasmids for $rcsA_{YPSTB}$ (pCBD253) and $rcsA_{YPE}$ (pCBD254) were made by PCR amplification from *Y. pseudotuberculosis* and *Y. pestis*, respectively, and cloning the products into pMal-c4x. RcsB with a C-terminal His_6 tag was purified by growing strain CDY475 at 26°C in LB medium with 100 mg/liter ampicillin to an OD_{600} of ~0.6. Arabinose (0.2%) was added to the culture, and growth was continued for 4 h before cells were harvested by centrifugation and stored at −80°C. Frozen cells were thawed, resuspended in buffer, and disrupted by sonication. The protein was then purified by using a Ni-nitrilotriacetic acid (NTA) His · Bind purification kit (Novagen), as recommended by the manufacturer. This single step provided RcsB-His_6 with greater than 80% purity, as assessed by SDS-polyacrylamide gel electrophoresis with Coomassie blue staining. MalE-$RcsA_{YPSTB}$ fusion and MalE-$RcsA_{YPE}$ fusion proteins were purified from strains carrying the expression plasmid pCBD253 or pCBD254, using the pMal purification system (New England BioLabs) following the manufacturer's protocols.

EMSA. For the electrophoretic mobility shift assay (EMSA), a 117-bp PCR product containing the RcsAB box or mutated RcsAB box of the *hmsT* promoter region was amplified using the primers shown in Table S1 in the supplemental material. Purified recombinant protein was added to DNA binding reaction mixtures containing 50 mM Tris-HCl (pH 7.5), 100 mM NaCl, 10 mM dithiothreitol (DTT), 500 μg/ml bovine serum albumin (BSA), and 35 ng PCR product. The binding assays were performed in a volume of 16 μl at room temperature for 30 min. After incubation, 4 μl of loading buffer (40% sucrose, 0.01% bromophenol blue, in binding buffer) was added, and the samples were electrophoresed at 70 V for 1 h in 6% DNA retardation gels (Invitrogen). The gels were stained with ethidium bromide.

RESULTS

The *Y. pestis* $rcsA_{YPSTB}$ biofilm defect is rescued by *hmsT* overexpression. In a previous study, we reported evidence that in *Y. pestis*, *rcsA* is a nonfunctional pseudogene, which we designated $rcsA_{YPE}$ (33). We showed that replacing $rcsA_{YPE}$ with the func-

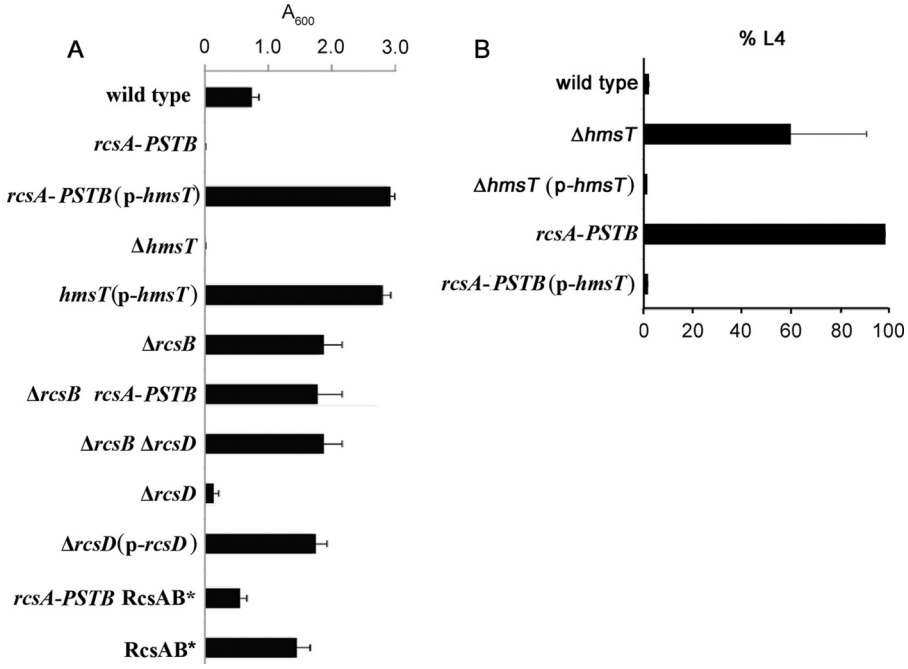

FIG 1 HmsT overexpression suppresses the biofilm defect of $RcsA_{YPSTB}$ expression. (A) *Y. pestis* biofilms produced in polystyrene culture dishes and quantified by crystal violet staining (Materials and Methods). The mean and standard deviation (SD) are indicated; all of the strains except for the $rcsA_{YPSTB}$ RcsAB* and RcsAB* strains differed significantly from the wild type ($P < 0.05$). (B) Biofilms adhering to the head of *C. elegans* were assayed for the ability to inhibit nematode growth by blocking feeding. Nematode eggs were deposited on *Y. pestis* lawns, and the fraction (mean ± SD) of animals developing to the fourth larval (L4) stage was scored (Materials and Methods).

tional *Y. pseudotuberculosis* allele ($rcsA_{YPSTB}$) resulted in strong loss of biofilms. In the reciprocal experiment, replacing the *Y. pseudotuberculosis* gene with the pseudogene allele, *Y. pseudotuberculosis* biofilm development was derepressed.

A hypothesis consistent with these results is that $RcsA_{YPSTB}$ represses transcription of the diguanylate cyclase gene *hmsT*, a known positive regulator of biofilms (4, 20, 32). If the hypothesis is correct, overexpressing *hmsT* in the *Y. pestis* $\Delta rcsA_{YPE}$::$rcsA_{YPSTB}$ ($rcsA_{YPSTB}$) background could be expected to restore biofilm production. We tested this with both *in vitro* and *in vivo* biofilm assays. In the *in vitro* assay, bacteria in growth medium are incubated in polystyrene dishes for approximately 24 h. After washing to remove planktonic bacteria, the adherent biofilm is stained with crystal violet, which is then solubilized and quantified. No biofilm was detectable in the *Y. pestis* $rcsA_{YPSTB}$ background (Fig. 1A). When the $rcsA_{YPSTB}$ strain was transformed with a high-copy *hmsT* plasmid, biofilms were restored, and in fact exceeded the wild-type level by about 4-fold. Essentially the same overproduction was observed when a biofilm-defective *hmsT* mutant was transformed with the *hmsT* overexpression plasmid.

Deleting *rcsB* in the $rcsA_{YPSTB}$ background also caused biofilm overproduction (Fig. 1A). This indicates that $RcsA_{YPSTB}$-mediated repression requires RcsB, consistent with the known functioning of Rcs phosphorelays (23) and our previous results (33). It also indicates that although *rcsA* is a pseudogene in *Y. pestis*, other genes encoding proteins of the Rcs phosphorelay are functional. In particular, the response regulator RcsB is capable of RcsA-independent repression.

In the *in vivo* assay, biofilms form on the nematode *C. elegans* and block the animal's feeding and development. Beginning with eggs at time zero, *C. elegans* normally develops to the fourth larval stage (L4) in 2 days at 20°C. Wild-type *Y. pestis* makes biofilms that prevent almost all worms from becoming L4s. An *hmsT* mutant had a strong, although somewhat variable, defect; plasmid overexpression restored growth inhibition to the wild-type level (Fig. 1B). In the same experiments, a strain with functional $rcsA_{YPSTB}$ substituted for the $rcsA_{YPE}$ pseudogene had a complete biofilm defect (i.e., all nematodes developed normally). Plasmid overexpression of *hmsT* fully rescued this defect. (If biofilm overproduction occurred it would not have been detected with this *in vivo* assay because wild-type *Y. pestis* completely inhibits nematode growth.)

The *in vitro* and *in vivo* experiments together suggest that *hmsT* is downstream of the Rcs phosphorelay and repressed by functional RcsA in an RcsB-dependent manner.

Rcs negatively regulates *Y. pestis hmsT* transcription. To further examine Rcs control of *hmsT*, we first deleted an endogenous *Y. pestis lacZ* gene (5) and then constructed transcriptional fusions using *E. coli lacZ* as the reporter. All fusions were integrated into the chromosome at their native locus.

We first compared two isogenic strains: one with the wild-type $rcsA_{YPE}$ pseudogene and the other with the $rcsA_{YPSTB}$ functional allele. Cells were grown in broth to mid-exponential, early stationary, and late stationary phases and were also grown overnight on agar and assayed for β-galactosidase activity. Under each growth condition, *hmsT*::*lacZ* transcription was strongly reduced in the $rcsA_{YPSTB}$ background (Table 2).

We next used the *hmsT*::*lacZ* reporter to determine the effects of overexpression of RcsB, $RcsA_{YPSTB}$, and $RcsA_{YPE}$. Overexpression of RcsB produced moderate decreases in *hmsT* transcription

TABLE 2 RcsB and RcsA-PSTB repression of *hmsT* transcription in *Y. pestis*

Y. pestis strain	Description[a]	β-Galactosidase activity (Miller units) under growth condition[b]: EP	ES	LS	Agar
CDY632	*hmsT*::*lacZ*	5.3 ± 1.4	5.9 ± 0.9	8.3 ± 1.6	9.5 ± 1.6
CDY1071	$rcsA_{YPSTB}$ *hmsT*::*lacZ*	**1.3 ± 0.2**[c]	**1.4 ± 0.2**[c]	**1.7 ± 0.3**[c]	**2.2 ± 0.4**[c]
CDY636	*hmsT*::*lacZ* (empty vector)	6.0 ± 1.4	7.1 ± 1.2	9.6 ± 1.9	9.8 ± 1.1
CDY637	*hmsT*::*lacZ* (p-*rcsB*)	4.2 ± 1.1	**4.1 ± 1.2**[d]	**4.0 ± 1.3**[d]	**4.1 ± 1.1**[d]
CDY640	*hmsT*::*lacZ* (empty vector)	5.4 ± 1.4	7.0 ± 1.4	6.1 ± 1.1	9.0 ± 1.6
CDY639	*hmsT*::*lacZ* (p-$rcsA_{YPSTB}$)	**1.3 ± 0.3**[e]	**1.4 ± 0.2**[e]	**0.9 ± 0.2**[e]	**1.4 ± 0.1**[e]
CDY638	*hmsT*::*lacZ* (p-$rcsA_{YPE}$)	6.7 ± 1.1	5.6 ± 1.1	6.8 ± 1.1	8.8 ± 1.1
CDY567	*hmsH*::*lacZ*	10.5 ± 1.6	11.0 ± 1.5	9.8 ± 2.5	11.1 ± 1.8
CDY568	$rcsA_{YPSTB}$ *hmsH*::*lacZ*	8.6 ± 1.4	8.8 ± 2.3	9.4 ± 1.6	9.5 ± 1.7
CDY614	*hmsP*::*lacZ*	1.8 ± 0.2	1.6 ± 0.1	1.8 ± 0.1	1.8 ± 0.1
CDY615	$rcsA_{YPSTB}$ *hmsP*::*lacZ*	1.7 ± 0.1	1.7 ± 0.6	1.7 ± 0.4	1.8 ± 0.1
CDY622	Δ*lacZ*	0.1 ± 0.1	0.2 ± 0.1	0.3 ± 0.1	0.2 ± 0.0

[a] All strains had deletion of the chromosomal *lacZ*. See Table 1 for further description of the plasmids.
[b] EP, exponential phase; ES, early stationary phase; LS, late stationary phase, 26°C, LB cultures; agar, colonies from LB agar plate incubated at 26°C for 24 h. Statistically significant differences are highlighted in boldface.
[c] $P < 0.01$ compared to CDY632.
[d] $P < 0.05$ compared to CDY636.
[e] $P < 0.01$ compared to CDY640.

under all conditions tested (Table 2); this is consistent with our previous study showing that RcsB overexpression reduces *in vitro* biofilms (33). Overexpression of functional $RcsA_{YPSTB}$ greatly decreased *hmsT* transcription, while the pseudogene-encoded $RcsA_{YPE}$ resulted in weak effects in both decreasing and increasing directions, suggestive of experimental noise.

To confirm the results of *lacZ* reporter assays, we used quantitative reverse transcription-PCR (qRT-PCR). Transcription of *hmsT* was strongly decreased when functional $rcsA_{YPSTB}$ was substituted for pseudogene $rcsA_{YPE}$ (Fig. 2). Deletion of *rcsB* in a strain with the pseudogene $rcsA_{YPE}$ produced a substantial increase in *hmsT* transcription over the wild-type level, suggesting that RcsB represses *hmsT* to some extent in the absence of functional RcsA. Deletion of *rcsD* repressed *hmsT* transcription, while double deletion of *rcsB* and *rcsD* produced an increase in transcription of *hmsT* (Fig. 2). This indicates that *rcsD* is functional and derepresses *hmsT* transcription through *rcsB*, consistent with the biofilm assays (Fig. 1A) (33).

We also examined HmsT expression by Western blotting. In *Y. pestis* with functional $rcsA_{YPSTB}$, HmsT was reduced to a nearly undetectable level (Fig. 3). When *rcsB* was deleted in the $rcsA_{YPSTB}$ background, expression was restored, further confirming that RcsA function requires RcsB. Consistent with the result that *hmsT* transcription was increased in an *rcsB* deletion strain (Fig. 2), HmsT expression also appeared to be slightly greater in the *rcsB* deletion strain (Fig. 3).

We used *lacZ* reporters to examine two other possible targets of $RcsA_{YPSTB}$ regulation. The operon *hmsHFRS* directs exopolysaccharide synthesis and is essential for *Y. pestis* and *Y. pseudotuberculosis* biofilms (10, 14, 15, 19). We assayed *hmsH*::*lacZ* transcriptional fusions to determine whether RcsA negatively regulates *hmsHFRS* (Table 2). Under all conditions tested, β-galactosidase was somewhat reduced in the $rcsA_{YPSTB}$ background, but this difference was not statistically significant, suggesting that Rcs has little direct effect on *hmsHFRS* expression. We also examined transcription of *hmsP*, encoding a c-di-GMP phosphodiesterase that negatively regulates biofilms. Transcription of an *hmsP*::*lacZ* fusion was unchanged in the $rcsA_{YPSTB}$ background, and plasmid overexpression of *rcsB* also did not affect *hmsP* transcription (Table 2). We conclude that *hmsP* is not an Rcs regulatory target.

RcsA represses *hmsT* in *Y. pseudotuberculosis*. We showed previously that *Y. pseudotuberculosis* strain IP32953 does not make biofilms in the *C. elegans* model, but will do so if its functional $rcsA_{YPSTB}$ is replaced by the *Y. pestis* pseudogene $rcsA_{YPE}$ (33). This suggested that, in *Y. pseudotuberculosis* as in *Y. pestis*, Rcs regulates *hmsT* transcription. We tested this with qPCR assays and Western blotting of the wild-type IP32953 strain and an isogenic

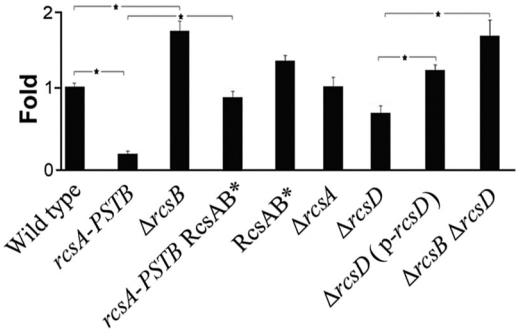

FIG 2 Effect of Rcs on *hmsT* transcription in *Y. pestis*. *hmsT* mRNA levels were determined by quantitative real-time PCR (Materials and Methods) and normalized to wild type. The means and standard deviations from three independent experiments with three replicates are indicated. *, $P < 0.05$.

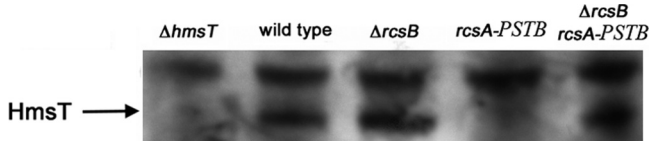

FIG 3 HmsT expression in *Y. pestis*. Western blots of total protein-matched lysates prepared from stationary-phase room temperature LB cultures and probed with polyclonal anti-HmsT antibody. The strain designations (Table 1) are as follows: Δ*hmsT*, CDY497; wild type, KIM6+; Δ*rcsB*, CDY326; *rcsA-PSTB* ($rcsA_{YPSTB}$), CDY330; and Δ*rcsB rcsA-PSTB* ($rcsA_{YPSTB}$), CDY421.

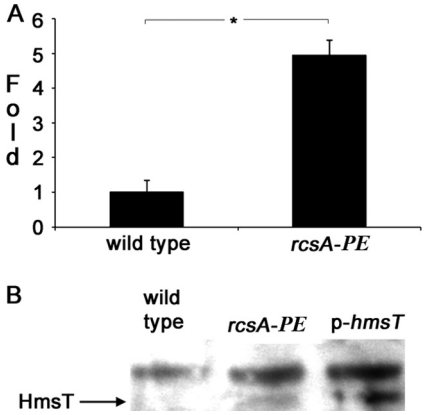

FIG 4 Effect of pseudogene $rcsA_{YPE}$ on *hmsT* expression in *Y. pseudotuberculosis*. Shown are relative amounts of *hmsT* mRNA (A) and HmsT protein (B) made by the wild type (IP32953) with a functional *rcsA* allele ($rcsA_{YPSTB}$) and the isogenic strain (CDY564) with the pseudogene ($rcsA_{YPE}$) replacement. The transcript level was determined by qRT-PCR as described in the legend to Fig. 2, and the protein level was determined by Western blotting as described in the legend to Fig. 3. The p-*hmsT* strain (CDY985) was included in panel B to allow the HmsT band to be distinguished from an unidentified cross-reacting protein.

$\Delta rcsA_{YPSTB}$::$rcsA_{YPE}$ ($rcsA_{YPE}$) substitution strain. Transcription of *hmsT* was increased 5-fold when the wild-type $rcsA_{YPE}$ allele was replaced by pseudogene $rcsA_{YPE}$ (Fig. 4A). In Western blotting, HmsT was undetectable in the wild type but was detected with the $rcsA_{YPE}$ substitution (Fig. 4B).

An RcsAB box in the *Y. pestis hmsT* promoter mediates downregulation. Using a PCR-based method (Materials and Methods), we determined the *hmsT* transcriptional start site to be 128 bp upstream of the initial ATG. The *hmsT* transcriptional start site is located in a palindromic RcsAB box that matches the consensus sequence at 12 of 14 nucleotides, including all 6 of the most conserved (34). The box is found at approximately the same position upstream of *hmsT* in all sequenced *Yersinia* spp. (see Table S2 in the supplemental material).

To determine whether Rcs transcriptional regulation acts on the RcsAB box, we mutated the box on the chromosome of wild-type and $rcsA_{YPSTB}$ *Y. pestis* strains by changing the CC dinucleotide to AG (designated RcsAB*). The mutation rescued the *in vitro* biofilm defect of the strain carrying functional $rcsA_{YPSTB}$ (Fig. 1A), and it restored *hmsT* transcription to the wild-type level (Fig. 2). These findings suggest that the mutation reduced or abolished binding by RcsB-$RcsA_{YPSTB}$.

***hmsT* promoter binding by RcsB alone and by RcsB with functional RcsA.** We directly assayed RcsB and RcsA binding to the RcsAB box using an electrophoretic mobility shift assay (EMSA). The DNA probe was a 117-bp promoter sequence comprising the RcsAB box and 38 bp 5′ and 65 bp 3′ of the box. RcsB was purified with a C-terminal His Tag, and RcsA was purified with an N-terminal MalE fusion. The promoter DNA was electrophoresed alone or after incubation with purified proteins (see Materials and Methods).

Purified RcsB retarded migration of the *hmsT* promoter in a concentration-dependent manner (Fig. 5A), indicating that RcsB binds the DNA without an accessory protein. This is consistent with genetic results (Fig. 2) suggesting that RcsB downregulates *hmsT* transcription.

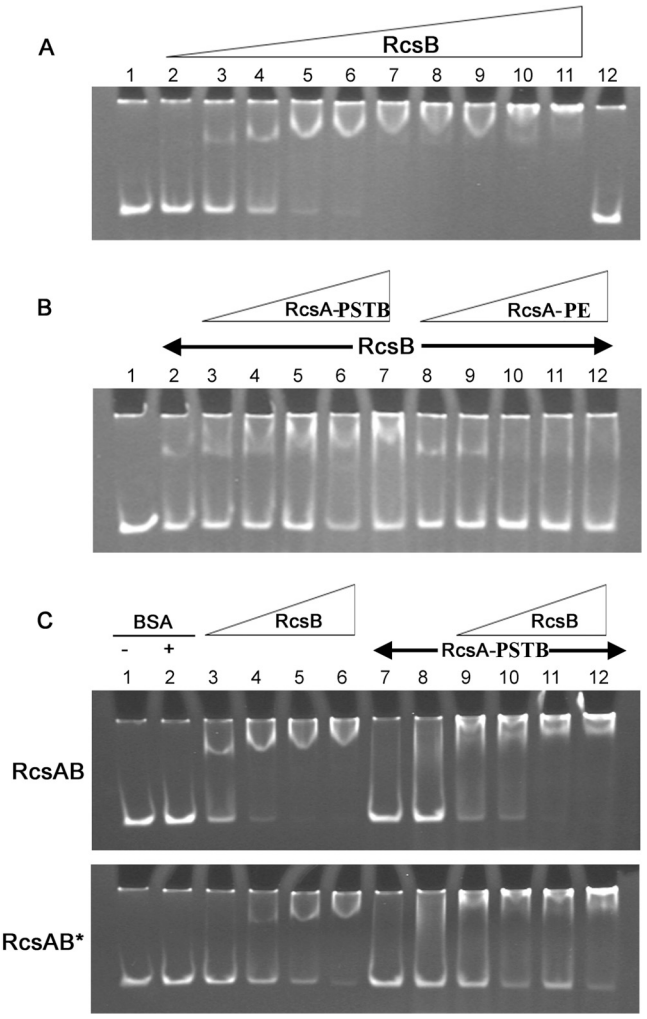

FIG 5 RcsB and RcsB-$RcsA_{YPSTB}$ bind the *hmsT* promoter. (A) Electrophoretic mobility shift assays (EMSAs) of *hmsT* promoter DNA incubated with increasing concentrations of RcsB. Lanes 1 and 12, *hmsT* probe alone; lanes 2 to 11, *hmsT* probe with 100, 200, 400, 600, 800, 1,000, 1,500, 2,000, 3,000, or 5,000 ng of RcsB in the 16-μl reaction mixture. (B) Supershift of *hmsT* promoter by $RcsA_{YPSTB}$ but not $RcsA_{YPE}$. Lane 1, *hmsT* probe alone; lanes 2 to 12, *hmsT* probe with 250 ng RcsB and with 250, 500, 1,000, 1,500, or 2,000 ng of $RcsA_{YPSTB}$ (lanes 3 to 7) or $RcsA_{YPE}$ (lanes 8 to 12).(C) RcsAB box mutation alters protein binding to the *hmsT* promoter. *hmsT* promoters with wild-type RcsAB box (top) or with the mutated RcsAB* box (bottom) were tested with identical protein combinations. Lanes 1 and 2, free *hmsT* probe in the absence or presence of bovine serum albumin (BSA); lanes 3 to 12 also contained BSA. Lanes 3 to 6 and 9 to 12 contained RcsB at 250, 500, 800, or 1,200 ng per reaction mixture; lanes 7 to 12 contained $RcsA_{YPSTB}$ at 2,000 ng (lane 7) or 3,000 ng (lanes 8 to 12) per reaction mixture.

$RcsA_{YPSTB}$ and $RcsA_{YPE}$ were used in the EMSA together with a fixed concentration of RcsB that produced a mobility shift. $RcsA_{YPSTB}$ with RcsB produced a concentration-dependent supershift of the promoter (Fig. 5B). $RcsA_{YPE}$ with RcsB did not supershift even at the maximum concentration tested (2,000 ng per 16-μl reaction). In fact, at high $RcsA_{YPE}$ concentrations the RcsB shift was almost undetectable (Fig. 5B, lanes 10 to 12). This suggests that the aberrant $RcsA_{YPE}$ accessory protein binds RcsB in a manner that prevents RcsB promoter binding.

In the absence of RcsB, $RcsA_{YPSTB}$ had no effect on mobility

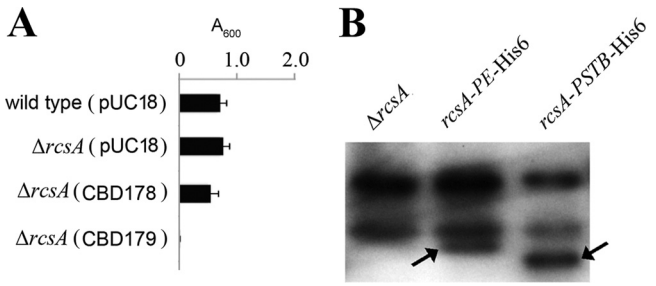

FIG 6 $RcsA_{YPE}$ does not have a biofilm-related regulatory function in *Y. pestis*. (A) Relative amounts of adherent biofilm made by *Y. pestis* KIM6+ derivatives. The mean and standard deviation from at least three independent experiments with three replicates are indicated. (B) Western blots of total protein-matched lysates prepared from stationary-phase room temperature LB cultures and probed with polyclonal anti-His antibody. As predicted from genome sequence data, $RcsA_{YPE}$ is 1 kDa bigger than $RcsA_{YPSTB}$ because of a 10-amino-acid internal duplication. Strain designations (Table 1) are as follows: Δ*rcsA*, CDY327; *rcsA-PE* ($rcsA_{YPE}$) SY743; and *rcsA-PSTB* ($rcsA_{PSTB}$), SY744.

even at very high concentrations (Fig. 5C, lanes 7 and 8). This is consistent with results for *E. coli* RcsA, which does not bind DNA in the absence of *E. coli* RcsB (23).

To examine binding specifically to the RcsAB box, we performed EMSA on both the wild-type and mutated boxes. With the wild-type box, 250 ng of RcsB was sufficient to produce a strong mobility shift, and at 500 ng, the free probe was almost undetectable (Fig. 5C, lanes 3 and 4). In contrast, with the mutated box, it required 800 ng of RcsB to produce a strong shift, and 1,200 ng for essentially complete shifting (Fig. 5C, lanes 5 and 6). The mutations also affected RcsB-$RcsA_{YPSTB}$ binding, which was assayed using a fixed amount (2,000 ng) of $RcsA_{YPSTB}$ and increasing concentrations of RcsB. With the wild-type RcsAB box, 800 ng of RcsB was sufficient to render the free probe undetectable (Fig. 5C, lane 11); with the mutated box, the free probe was still detectable even with 1,200 ng of RcsB (Fig. 5C, lane 12).

***rcsA* is not a biofilm-related gene in *Y. pestis*.** The above EMSA results showed $RcsA_{YPE}$ prevents RcsB binding to *hmsT* promoter (Fig. 5B). However, deletion or overexpression of $rcsA_{YPE}$ did not affect biofilm formation or *hmsT* transcription in *Y. pestis* (Fig. 1A, 2, and 6A and Table 2), indicating that $rcsA_{YPE}$ is a nonfunctional pseudogene. One explanation for the apparent discrepancy is that $RcsA_{YPE}$ is not expressed *in vivo*. To test this and due to the absence of an RcsA antibody, plasmids expressing $RcsA_{YPSTB}$-His_6 and $RcsA_{YPE}$-His_6 were constructed. Addition of a His_6 tag on the C terminus of RcsA did not affect the role of $RcsA_{YPSTB}$ or $RcsA_{YPE}$ (data not shown). Expression of $RcsA_{YPE}$ and $RcsA_{YPSTB}$ was further analyzed by immunoblotting. As shown in Fig. 6B, both $RcsA_{YPE}$ and $RcsA_{YPSTB}$ proteins were detected. Taken together, these results suggested $RcsA_{YPE}$ can be expressed *in vivo*, but it does not function to downregulate *hmsT*.

DISCUSSION

Y. pestis and *Y. pseudotuberculosis* diverged from a common ancestor within the past 20,000 years (1, 2). Despite many genetic and genomic similarities, the two have markedly different life cycles (6, 21, 26, 30). *Y. pestis* exists enzootically, shuttling between rodents and their fleas, and because of multiple auxotrophies is apparently an obligate parasite. *Y. pseudotuberculosis* is a prototroph capable of life outside a host, and is often found in association with warm-blooded animals. As a pathogen, *Y. pseudotuberculosis* is infectious orally; it has no known invertebrate vector and was unable to block fleas in extensive tests (13).

We previously obtained evidence suggesting that, during the evolution of *Y. pestis*, *Y. pestis rcsA* mutated from a functional allele ($rcsA_{YPSTB}$) to a pseudogene ($rcsA_{YPE}$) was the product of natural selection and not genetic drift (33). The mutation apparently was required for *Y. pestis* to colonize its flea vector with a biofilm, because *Y. pestis* in which $rcsA_{YPSTB}$ was substituted for $rcsA_{YPE}$ were strongly defective for flea blockage (33).

In the present study, we show that a target of Rcs regulation is *hmsT*, encoding a DGC that regulates biofilms. Several lines of evidence support this conclusion. First, in both *in vivo* and *in vitro* assays, *hmsT* overexpression restores biofilms to *Y. pestis* expressing $rcsA_{YPSTB}$ (Fig. 1). Second, *hmsT* transcription is reduced when $rcsA_{YPSTB}$ is present in the cells (Table 2 and Fig. 2), and HmsT protein levels are also reduced (Fig. 3). Consistent with the *Y. pestis* results, when pseudogene $rcsA_{YPE}$ was placed in *Y. pseudotuberculosis*, *hmsT* transcription was markedly increased, and HmsT protein became detectable (Fig. 4); the same substitution conferred biofilm competence in the *C. elegans* assay to a *Y. pseudotuberculosis* strain that did not otherwise form detectable biofilms in that system (33). Third, *hmsT* transcription is reduced in an *rcsD* deletion strain, while *hmsT* transcription is increased in an *rcsB* and *rcsD* double deletion strain (Fig. 2). Finally, we showed that RcsB alone, or RcsB combined with $RcsA_{YPSTB}$, binds the *hmsT* promoter, while $RcsA_{YPSTB}$ alone does not (Fig. 5).

$RcsA_{YPE}$ prevents RcsB binding to *hmsT* promoter *in vitro* (Fig. 5B) and can be expressed in *Y. pestis* (Fig. 6B), but it did not have a biofilm-related function under our tested conditions (Fig. 1A, 2, and 6B and Table 2), indicating $rcsA_{YPE}$ is a pseudogene rather than a functional mutant allele. However, we cannot preclude the possibility that $RcsA_{YPE}$ plays a role under a specific environmental condition or in other Rcs-regulated phenotypes.

It has been reported that Rcs system negatively regulates *flhDC* transcription in *Escherichia coli* (16). An RcsAB box is present at 4 bp downstream of the transcription start site of the *flhDC* gene, and RcsAB heterodimer binding to the box might prevent the RNA polymerase from binding to the promoter (16). In *Yersinia* spp., the *hmsT* transcription start site is located in the RcsAB box; thus, the Rcs system might use a similar mechanism to repress *hmsT* transcription in *Y. pestis*.

A previous report on *Y. pseudotuberculosis* Rcs by Hinchliffe et al. produced evidence that Rcs positively regulates biofilms *in vitro* (18). This appears to contradict our findings, both in the present study (Fig. 1) and in previous results (33), that Rcs negatively regulates biofilms. The reasons for this discrepancy are uncertain, but it is significant that the study by Hinchliffe et al. reported robust biofilm formation at 37°C (18). In both *Y. pestis* (20) and *Y. pseudotuberculosis* (C. Darby, unpublished data), biofilms that require the *hmsHFRS* exopolysaccharide operon and *hmsT* biofilms have been shown to be downregulated at 37°C. The study by Hinchliffe et al. did not report whether the biofilms observed were dependent on either *hmsT* or *hmsHFRS*. It is possible then, that the observed Rcs-dependent biofilms are not *hmsT* or *hmsHFRS* dependent, i.e., that *Y. pseudotuberculosis* has multiple means of making biofilms under different environmental conditions.

Y. pestis hmsT mutation and *Y. pestis* $rcsA_{YPSTB}$ strains have similar biofilm phenotypes *in vitro* but different biofilm phenotypes *in vivo*. *Y. pestis* $rcsA_{YPSTB}$ forms almost no biofilm on the

head of *C. elegans* or in the digestive tract of fleas, whereas the *Y. pestis hmsT* mutant forms intermediate levels of biofilm on the head of *C. elegans* and in the digestive tract of the flea (Fig. 1B) (32). Thus, repressing *hmsT* is not the only mechanism by which Rcs negatively regulates biofilms. Rcs may regulate other target genes to repress *Yersinia* biofilm formation.

Our data support a model of multilevel control of *hmsT* and thus of biofilms. In the presence of RcsB and functional RcsA, as is found in *Y. pseudotuberculosis*, *hmsT* transcription is tightly repressed. Presumably *Y. pseudotuberculosis* has mechanisms to relieve this repression under appropriate conditions, but the place of biofilms in the *Y. pseudotuberculosis* life cycle is not known. This tight repression apparently was partially relieved during *Y. pestis* evolution by the conversion of *rcsA* to a pseudogene (33). There remains a residual repression mediated by Rcs, as indicated by the fact that *Y. pestis rcsB* deletion strains overproduce biofilms and the *rcsD* deletion strain produces decreased biofilms. The reason for the apparent continuing need for Rcs is uncertain. It is possible that the biofilm overproduction that occurs when *rcsB* is deleted reaches an extent that the insects would no longer perform as well as vectors, implying selection to maintain *rcsB.* Furthermore, deletion of either *rcsC* or *rcsD* in *Y. pseudotuberculosis* resulted in defects in adhesion to, and invasion of, a human epithelial cell line (18), suggesting that the Rcs phosphorelay also functions during mammalian infection. If also true in *Y. pestis*, this would preclude mutation of *rcsB* as an adaptive step in *Y. pestis* evolution. In summary, then, it appears that *Y. pestis* evolved to occupy the flea niche in part by derepressing *hmsT*, thereby derepressing biofilms.

ACKNOWLEDGMENTS

We thank Alexandra Koumoutsi for assistance with strain construction.

This work was supported by NIH grant AI057512 (to C.D.); the Division of Intramural Research, National Institute of Allergy and Infectious Diseases (NIAID), National Institutes of Health (NIH), and by the Institute of Pathogen Biology, Chinese Academy of Medical Sciences.

REFERENCES

1. **Achtman M, et al.** 2004. Microevolution and history of the plague bacillus, *Yersinia pestis.* Proc. Natl. Acad. Sci. U. S. A. **101**:17837–17842.
2. **Achtman M, et al.** 1999. *Yersinia pestis*, the cause of plague, is a recently emerged clone of *Yersinia pseudotuberculosis.* Proc. Natl. Acad. Sci. U. S. A. **96**:14043–14048.
3. **Bobrov AG, et al.** 2011. Systematic analysis of cyclic di-GMP signalling enzymes and their role in biofilm formation and virulence in *Yersinia pestis.* Mol. Microbiol. **79**:533–551.
4. **Bobrov AG, Kirillina O, Forman S, Mack D, Perry RD.** 2008. Insights into *Yersinia pestis* biofilm development: topology and co-interaction of Hms inner membrane proteins involved in exopolysaccharide production. Environ. Microbiol. **10**:1419–1432.
5. **Bobrov AG, Perry RD.** 2006. *Yersinia pestis lacZ* expresses a beta-galactosidase with low enzymatic activity. FEMS Microbiol. Lett. **255**: 43–51.
6. **Brubaker RR.** 1991. Factors promoting acute and chronic diseases caused by yersiniae. Clin. Microbiol. Rev. **4**:309–324.
7. **Chain PS, et al.** 2004. Insights into the evolution of *Yersinia pestis* through whole-genome comparison with *Yersinia pseudotuberculosis.* Proc. Natl. Acad. Sci. U. S. A. **101**:13826–13831.
8. **Darby C.** 2008. Uniquely insidious: *Yersinia pestis* biofilms. Trends Microbiol. **16**:158–164.
9. **Darby C, Ananth SL, Tan L, Hinnebusch BJ.** 2005. Identification of *gmhA*, a *Yersinia pestis* gene required for flea blockage, by using a *Caenorhabditis elegans* biofilm system. Infect. Immun. **73**:7236–7242.
10. **Darby C, Hsu JW, Ghori N, Falkow S.** 2002. *Caenorhabditis elegans:* plague bacteria biofilm blocks food intake. Nature **417**:243–244.
11. **Datsenko KA, Wanner BL.** 2000. One-step inactivation of chromosomal genes in *Escherichia coli* K-12 using PCR products. Proc. Natl. Acad. Sci. U. S. A. **97**:6640–6645.
12. **Donnenberg MS, Kaper JB.** 1991. Construction of an *eae* deletion mutant of enteropathogenic *Escherichia coli* by using a positive-selection suicide vector. Infect. Immun. **59**:4310–4317.
13. **Erickson DL, Jarrett CO, Wren BW, Hinnebusch BJ.** 2006. Serotype differences and lack of biofilm formation characterize *Yersinia pseudotuberculosis* infection of the *Xenopsylla cheopis* flea vector of *Yersinia pestis.* J. Bacteriol. **188**:1113–1119.
14. **Fetherston JD, Schuetze P, Perry RD.** 1992. Loss of the pigmentation phenotype in *Yersinia pestis* is due to the spontaneous deletion of 102 kb of chromosomal DNA which is flanked by a repetitive element. Mol. Microbiol. **6**:2693–2704.
15. **Forman S, et al.** 2006. Identification of critical amino acid residues in the plague biofilm Hms proteins. Microbiology **152**:3399–3410.
16. **Francez-Charlot A, et al.** 2003. RcsCDB His-Asp phosphorelay system negatively regulates the *flhDC* operon in *Escherichia coli.* Mol. Microbiol. **49**:823–832.
17. **Gerlach RG, Holzer SU, Jackel D, Hensel M.** 2007. Rapid engineering of bacterial reporter gene fusions by using Red recombination. Appl. Environ. Microbiol. **73**:4234–4242.
18. **Hinchliffe SJ, Howard SL, Huang YH, Clarke DJ, Wren BW.** 2008. The importance of the Rcs phosphorelay in the survival and pathogenesis of the enteropathogenic yersiniae. Microbiology **154**:1117–1131.
19. **Jarrett CO, et al.** 2004. Transmission of *Yersinia pestis* from an infectious biofilm in the flea vector. J. Infect. Dis. **190**:783–792.
20. **Kirillina O, Fetherston JD, Bobrov AG, Abney J, Perry RD.** 2004. HmsP, a putative phosphodiesterase, and HmsT, a putative diguanylate cyclase, control Hms-dependent biofilm formation in *Yersinia pestis.* Mol. Microbiol. **54**:75–88.
21. **Koornhof HJ, Smego RA, Jr, Nicol M.** 1999. Yersiniosis. II. The pathogenesis of *Yersinia* infections. Eur. J. Clin. Microbiol. Infect. Dis. **18**:87–112.
22. **Lillard JW, Jr, Bearden SW, Fetherston JD, Perry RD.** 1999. The haemin storage (Hms+) phenotype of *Yersinia pestis* is not essential for the pathogenesis of bubonic plague in mammals. Microbiology **145**:197–209.
23. **Majdalani N, Gottesman S.** 2005. The Rcs phosphorelay: a complex signal transduction system. Annu. Rev. Microbiol. **59**:379–405.
24. **Miller JH.** 1972. Experiments in molecular genetics. Cold Spring Harbor Laboratory, Cold Spring Harbor, NY.
25. **Perry RD, et al.** 2004. Temperature regulation of the hemin storage (Hms+) phenotype of *Yersinia pestis* is posttranscriptional. J. Bacteriol. **186**:1638–1647.
26. **Prentice, MB, Rahalison L.** 2007. Plague. Lancet **369**:1196–1207.
27. **Ross P, et al.** 1990. The cyclic diguanylic acid regulatory system of cellulose synthesis in *Acetobacter xylinum.* Chemical synthesis and biological activity of cyclic nucleotide dimer, trimer, and phosphothioate derivatives. J. Biol. Chem. **265**:18933–18943.
28. **Ross P, et al.** 1987. Regulation of cellulose synthesis in *Acetobacter xylinum* by cyclic diguanylic acid. Nature **324**:279–281.
29. **Sebbane F, Jarrett CO, Gardner D, Long D, Hinnebusch BJ.** 2006. Role of the *Yersinia pestis* plasminogen activator in the incidence of distinct septicemic and bubonic forms of flea-borne plague. Proc. Natl. Acad. Sci. U. S. A. **103**:5526–5530.
30. **Smego RA, Frean J, Koornhof HJ.** 1999. Yersiniosis. I. Microbiological and clinicoepidemiological aspects of plague and non-plague *Yersinia* infections. Eur. J. Clin. Microbiol. Infect. Dis. **18**:1–15.
31. **Sun YC, Koumoutsi A, Darby C.** 2009. The response regulator PhoP negatively regulates *Yersinia pseudotuberculosis* and *Yersinia pestis* biofilms. FEMS Microbiol. Lett. **290**:85–90.
32. **Sun YC, et al.** 2011. Differential control of *Yersinia pestis* biofilm formation *in vitro* and in the flea vector by two c-di-GMP diguanylate cyclases. PLoS One **6**:e19267.
33. **Sun YC, Hinnebusch BJ, Darby C.** 2008. Experimental evidence for negative selection in the evolution of a *Yersinia pestis* pseudogene. Proc. Natl. Acad. Sci. U. S. A. **105**:8097–8101.
34. **Wehland M, Bernhard F.** 2000. The RcsAB box. Characterization of a new operator essential for the regulation of exopolysaccharide biosynthesis in enteric bacteria. J. Biol. Chem. **275**:7013–7020.
35. **Yanisch-Perron C, Vieira J, Messing J.** 1985. Improved M13 phage cloning vectors and host strains: nucleotide sequences of the M13mp18 and pUC19 vectors. Gene **33**:103–119.